Exploring Structural, Spectroscopic, Optical, Morphological, Mechanical, Antibacterial And Thermal Parameters Of Glycine A.R Single Crystals For Advanced Optoelectronics, Photonics, Laser Components And Non Linear Optical Applications

N.Rajasekar¹, K. Balasubramanian^{2*}

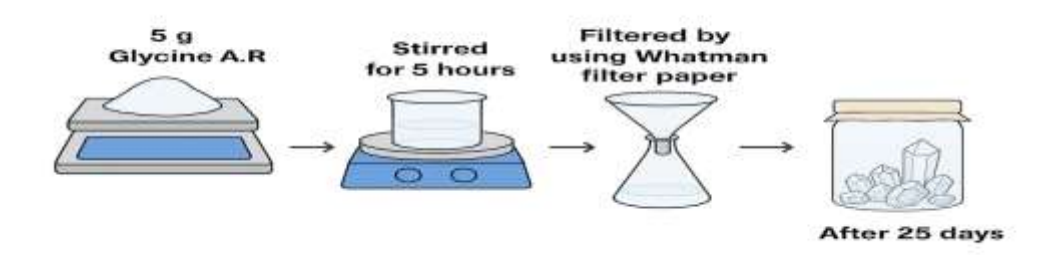
¹Research scholar (Reg.No: 22211072131006), PG and Research department of physics, The M.D.T Hindu college, Pettai, Tirunelveli-627010, Tamilnadu, India.

^{2*}Associate professor, PG and Research department of physics, The M.D.T Hindu college, Pettai, Tirunelveli-627010, Tamilnadu, India.

^{1,2*}Affillated by ManonmaniamSundarnar University, Abishekapatti-627012, Tirunelveli, Tamilnadu, India.

Corresponding author. Correspondence: K. Balasubramanian E-mail: *rs9012618@gmail.com

Graphical abstract



Abstract

Glycine A.R was obtained via the slow evaporation method employing deionized water under ambient temperature. Powder X ray diffraction confirmed a Hexagonal structure which has assigned to P2₁/c. Powder XRD measurements was employed, and the Hall equation method was applied to evaluate crystallite size (d) and lattice strain (η) of the material. The distinct vibrational bands and assignments are present in the FTIR spectroscopy. Uv-vis analysis the wavelength versus Absorbance (A.U), Transmittance (%) and Tauc plot revealed that 4.58 eV and optical parameters such as Refractive index, Reflectance (%), Extinction coefficient and Optical conductivity are observed. Thermal stability of Glycine A.R was examined using TG-DTA under controlled heating under nitrogen ambience with a constant heating rate to identify dehydration and decomposition process. The broido's method was employed to evaluate kinetic properties comprising (ΔS), (ΔH), and (ΔG) of decomposition. Scanning electron microscopy is observed to the Morphological and particle size. EDX analysis is to find the Carbon, Nitrogen and oxygen the various types atomic constituents elements existing in the compound. The CHN studies revealed three constituents, namely Carbon (%), Hydrogen (%) and Nitrogen (%). The Photoluminescence spectrum of the sample exhibited an intense maximumpeak around 466 nm, which corresponds to anoptical Bandgap possessing 2.66 eV. The crystal exhibited a LDT measurements revealed that the crystal can withstand a maximum intensity of 22.2 GW/cm². The NLO characteristics of Glycine A.R single crystalswas investigated through the Z-scan techniquefor evaluating its nonlinearthird order susceptibilty $(\chi^{(3)})$ is calculated as 1.33 x 10⁻¹³esu. In ¹H FT-NMR analysis verified the chemical configuration. Vickers hardness measurements were performed for thesynthesized crystal to evaluate its mechanical properties. mayer's indexnumber was found to be n is 4.33, confirming a hard which favorable classification as material. for nonlinear optical applications.characterization of synthesizedspecimens demonstrate potential applicabilityinLaser components, photonic, opto electronic device and nonlinear optical applications. The results revealed no inhibition zones for the tested bacterial strains, confirming the absence of antibacterial activity in the material.

Keywords: Slow evaporation method, Structural, Hall-Williamson Plot, Spectroscopic, Optical, thermal kinetic parameters - Broido's and Kissinger methods, mechanical and Antibacterial analysis; S. aureus; E. coli; crystal growth; bio-inactivity

Material synthesis

Glycine A.R (molecular weight: 70.07) was used as the material for crystal growth experiments. Glycine A.R was synthesis at room temperature. The Glycine A.R was taken as (5gm) in weighing mechine and then dissolved with less than 50 ml deionized water in a beaker. Then, solution in the glass beaker was mixed using a magnetic stirrer over continously 5 hours. Later, the beaker underwent filtration with whatmann filter paper. The settled microdust and impurities are well cleaned. The solution was kept under the dust free place for nucleation and it take time harvesting period of 25days.

The molecular formula for Glycine A.R is C₂H₅NO₂



Fig. 1. Photographic picture of Glycine A.R single crystals

Introduction

Most amino acidsexhibit potential for NLO applications. Glycine is the simplest amino acids which is used as a additive in protein. Analytical reagent grade (A.R) glycine is commonly used to grow high-quality single crystals, which are ideal for studying optical and electronic properties. It can influence crystal growth, Lattice formation, Opto electronics and NLO [1-4]. The Glycine exists in three polymorphic forms (α, β, γ) with one form exhibiting crystal growth of amino acid-based crystals. Glycine due to its crystalline form and zwitterionic nature several used for nonlinear optical material research. In powder XRD glycine has unit cell determination of a = 5.04 A° , b = 12.1 A° , c = 5.41 A° , V = 305.25 and Z = 4, the three angles are $\alpha = 90^{\circ}$, $\beta = 112.3^{\circ}$, $\gamma = 90^{\circ}$. The crystal system has monoclinic in structure which is space group of P2₁/c with a primitive lattice. X-Ray diffraction (XRD) analysis of the synthesized glycine A.R confirmed that the observed peaks correspond to the Glycine crystal structure. The centro-symmeteric and non centrosymmetric both can exhibit third harmonic generation. In, FTIR the presence variety of Peaks corresponds to different vibrational modes, allowing the identification and assignment of specific functional moieties within the compound. In the research paper describe the crystallization of Glycine in the aqueous solution at room temperature. In this Glycine A.R single crystal the various analyze of P-XRD, FTIR, UV-vis, SEM, EDX, CHN, Microhardness, Flurouscenes, TG-DTA, ¹H FT-NMR, LDT, Antibacterial and Z scan.

In this research paper the Glycine A.R mainly used as a candidate for third order NLO applications includes self focusing, Laser systems, and Remote sensing technologies these applications are indirectly relevant to telecommunications, Defence and space Research.Nonlinear optics is being explored in Primarily for its potential in enabling efficient frequency conversion, Optical switching, and signal processing in modern photonic technology [5].

Results and discussion

1). P-XRD investigation

X-ray powder analysisserves for identifying the crystalline structure in powdered form. In powder XRD we determine unit cell dimensions, Phase identification crystallinearrangement. Crystallinity, phase compositionalong with structural parameters associated with the developed specimen was studied via PXRD with cuk α radiation ($\lambda = 1.5418$ A°). Glycine A.Rwere analyzed within the angular interval between $5^{\circ} - 10^{\circ}$ (20) with a step increment of 0.05 per minute. Phase identification determining the compounds by matching the pattern with database like JCPDS-ICCD. The standard values for determining unit cell dimensionswerea = 5.04 A° , b = 12.1 A° , c = 5.41 A° , V = 305.25 A^{3} and Z = 4, the three angles are $\alpha = 90^{\circ}$, $\beta = 112.3^{\circ}$, $\gamma = 90^{\circ}$. The Glycine A.R forms a centrosymmetric P2₁/clattice exhibiting a monoclinic structure with a primitive lattice. The various peaks observed at different (h k l) values are (020), (110), (120), (040), (140), (211), (200), (032), (222) and (260). The maximum peak obtained at (25.358° Degree). The standard database Glycine A.R values are observed by using the ICCD –JCPDS card number is (07-0718).

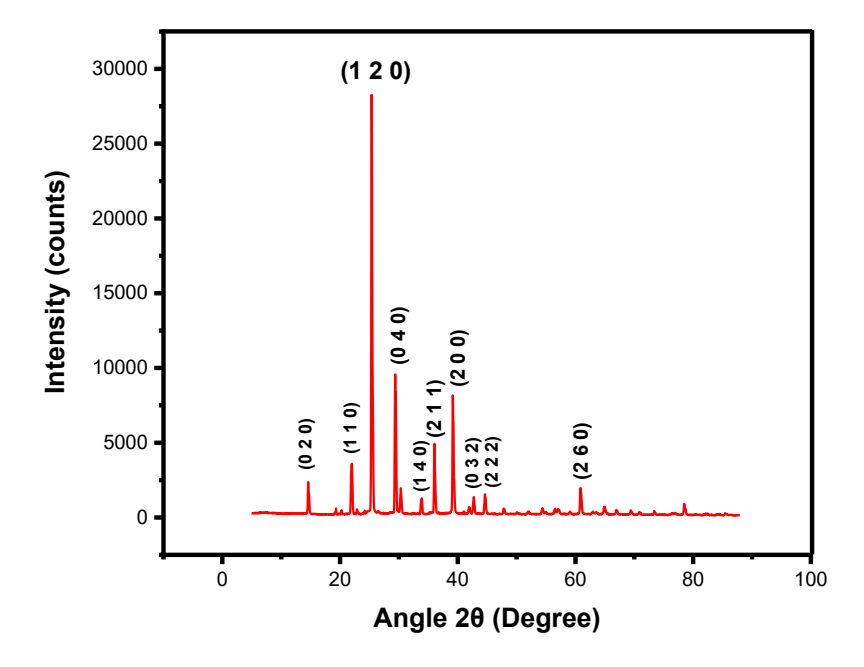


Fig. 2 (a) Powder XRD Pattern of the sample

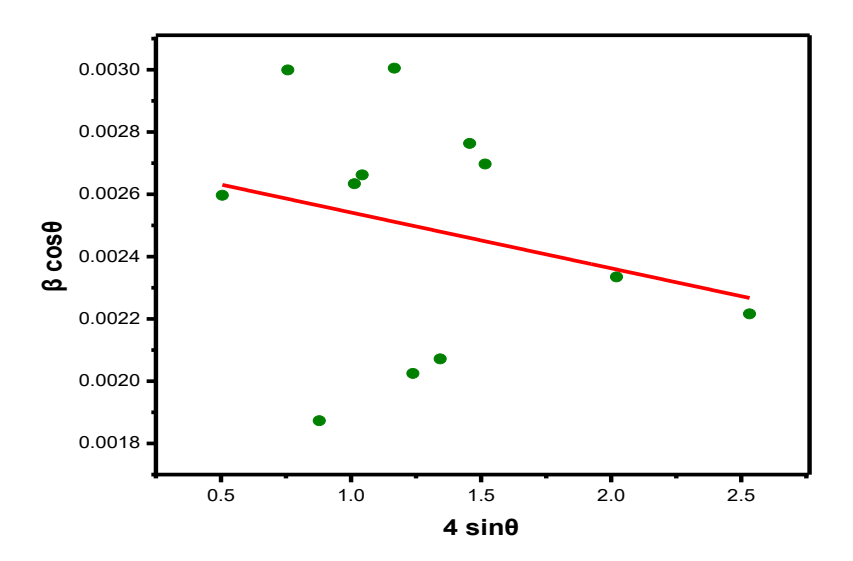


Fig. 2 (b) Williamson Hall plot of Glycine A.R

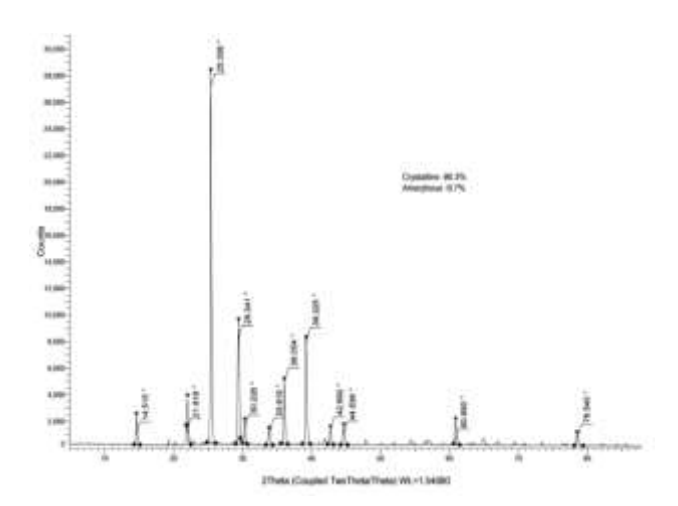


Fig.2 (c) XRD spectra of the synthesized crystal

Table. 1

Angle Relative intensity d spacing FWHM Left [2th.]

(20 degree)	(%)		
14.515 °	2.5%	6.09747 Å	0.150 °
21.818 °	3.4%	4.07035 Å	0.175 °
25.358 °	100.0%	3.50949 Å	0.110°
29.341 °	29.4%	3.04151 Å	0.156 °
30.226 °	4.3%	2.95442 Å	0.158 °
33.915 °	3.7%	2.64110 Å	0.180 °
36.054 °	17.7%	2.48916 Å	0.122 °
39.225 °	28.9%	2.29488 Å	0.126 °
42.692 °	3.8%	2.11620 Å	0.170 °
44.536 °	2.6%	2.03277 Å	0.167 °
60.690°	0.4%	1.52472 Å	0.155 °
78.540 °	2.1%	1.21695 Å	0.164 °

The williamson- Hall method was applied to analyze the peak broadening observed in the XRD profile, allowing a combined evaluation of crystallite size and lattice strain.

The W-H equation is employed to evaluate the microstrain (η) in the crystal lattice.

$$\beta \cos\theta = K\lambda/D + 4\eta Sin\theta \tag{1}$$

The intercept obtained from the Williamson-Hall analysis was determined as 0.00272, which reflects the influence of crystallite size on the diffraction line broadening.

From the linear fitting of the Williamson-Hall plot, the lattice strain of the material was estimated as 1.79×10^{-4} , suggesting a minor tensile strain within the crystalline lattice.

Using the Debye-scherrer equation, the crystallite size of Glycine A.R was calculated

$$D = K\lambda / \beta \cos\theta(2)$$

Based on the slope-intercept relationship of the Williamson-Hall plot, the mean crystallite dimension for this sample has been determined to be approximately 51 nm, confirming the nanocrystalline nature of the material.

The dislocation density, indicating the number structural irregularities in a lattice framework, were analyzed through a relation $\delta = 1/D^2$. The result, approximately 3.85 x 10^{10} cm⁻², suggests a moderate level of dislocations in the material [6].

Table. 2 Structural parameters of Glycine A.R single crystals

Description	Result			
Highest peak	(2θ) 25.287			
FWHM (β)	0.0029 radians			
Intercept value of b	0.00272			
Strain (η)	1.79 x 10 ⁻⁴			
Crystalline size (D)	51 nm			
Dislocation density	$3.85 \times 10^{10} \text{ cm}^{-2}$			
Crystallinepercentage	90.3 (%)			

2). FTIR analysis

There are various modes were analyzed usingFTIR spectroscopy. Thus, observed IR peak around 499.65 cm⁻¹ correspond to C-C-C bending (backbone), whereas the peak near 604.30 cm⁻¹ corresponds to Bending/deformation associated with C-C-N bending, Furthermore, the 666.34 cm⁻¹ peak corresponds to -CH₂⁺ rocking (out of plane bending). The 681.25 cm⁻¹ peak arises from the CH₂ rocking.

A band obtained around 891.58 cm⁻¹ corresponds to Stretching/bending vibrations, while 930.57 cm⁻¹ arises from wagging/torsion (CH₂ wagging). The band at 1045.48 cm⁻¹ represents deformation in C-N stretching (amine group).

A peak around 1121.41 cm⁻¹arises from Rocking/stretching mode of CH₂rocking. Thus, the 1322.50 cm⁻¹peak representsCH₂ wagging (methylene group). The1390.21 cm⁻¹ peak corresponds to Symmetric COO- stretching vibrations. The 1437.41 cm⁻¹ peak corresponds to COO-asymmetric vibration (overlapping). The peak produced 1485.63 cm⁻¹ is arises from Ammonium group (NH₃+ asymmetric bending vibrations). The 1571.81 cm⁻¹band represents Asymmetric COO- stretching. A peak appearing at 2759.91 cm⁻¹ corresponds to CH stretching

vibrations[7, 8]. Thus,Fig (3) denotes the FTIR graph spectrum. Table. (3) listed the Wavelength and various assignments to the functional groups

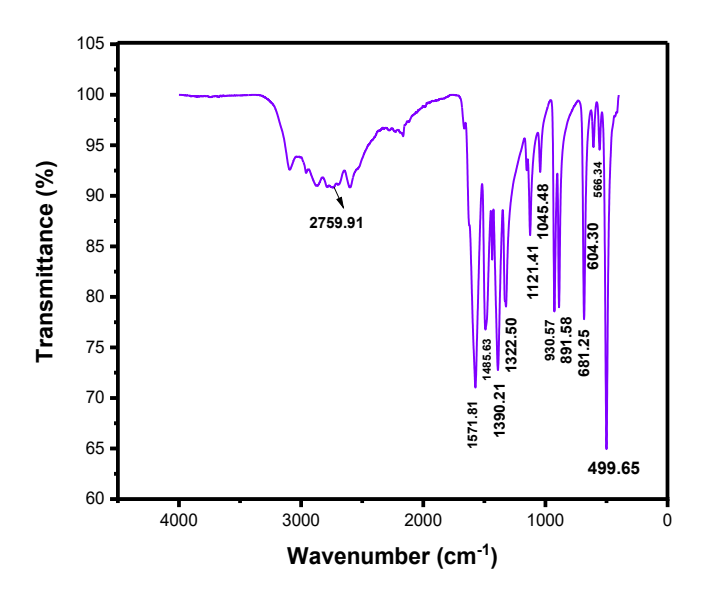


Fig. 3 FTIR spectrum of Glycine A.R

Table. 3 Thevibrational bands, Assignment type and chemical moiety

Vibrational bands (cm ⁻¹)	Assignment type	chemical moiety	
499.65	Bending/ skeletal vibration	C-C-C bending (backbone)	
604.30	Bending/deformation	C-C-N bending	
666.34	out of plane bending	-CH ₂ ⁺ rocking	
681.25	Bending/deformation CH ₂ I	Rocking	
891.58 Stretching/bending	C-C stretching		
930.57 Stretching	C-C stretching (backbone	·)	
1045.48	C-N stretching	C-N stretching (amine group)	
1121.41 C-O/C-N stretching C-O stretching (carboxylic acid)			
1322.50 CH ₂ bending/waggingCH ₂ wagging (methylene group)			

1390.21	Symmetric COO- stretching	ngCarboxylate group (-COO symmetric)
1437.41	CH ₂ bending	COO-asymmetric stretching (overlap)
1485.63NH ₃ ⁺	bending Ammonium	group (NH ₃ + asymmetric bending)
1571.81	Asymmetric COO- stretching	Carboxylate group (COO- asymmetric)
2759.91	CH stretchingA	Aldehydic CH (-CHO).

3). Uv- vis analysis

In, Uv-vis analysis the wavelength were recorded within the range is 200 nm-800nm. The wavelength versus absorbance graph the absorption arises from electronic excitations or conjucated carbonyl (or) aromatic group, contributes to $(\pi - \pi^*)$ transitions. Glycine A.R crystal shows a transparency of 61 %. The transmittance vs wavelength lower cutoff frequency is 231 nm, indicating carbonyl (c=0) functionality within the -CONH₂ (amide) group due to $(n-\pi^*)$ transitions [9].

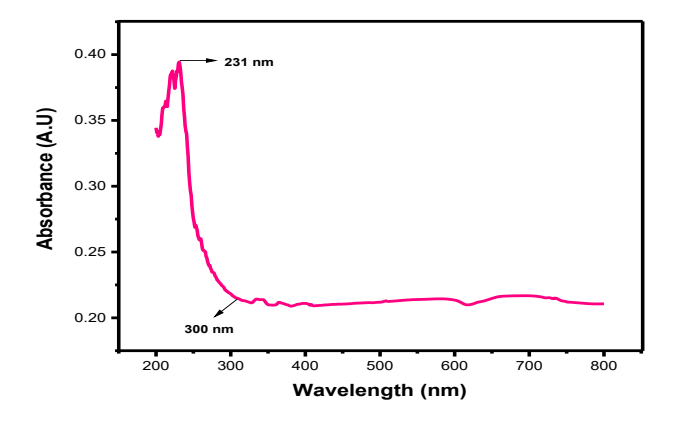


Fig. 4 (a) Wavelength versus absorbance

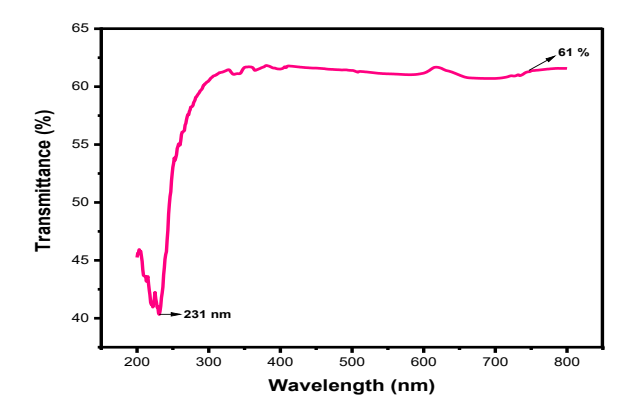


Fig. 4(b) Wavelength versus Transmittance

Absorption coefficientbased on the following equation is,

$$\alpha = 2.303 \text{ x Absorbance/t (cm}^{-1})$$
 (3)

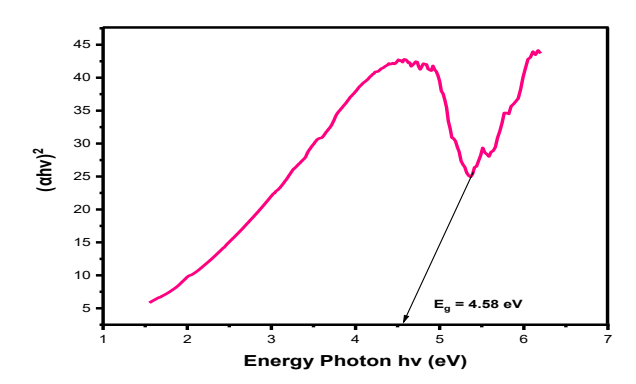


Figure. 4(c) Energy Photon hv (eV) versus (αhv)²

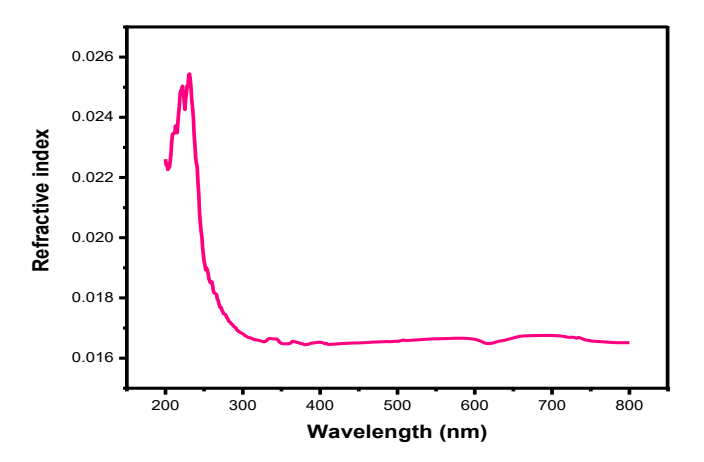
The energy of the photon is,

$$E_{g} = hc / \lambda c \tag{4}$$

The direct bandgap energy was using this relation is

$$(\alpha h v)^2 = \alpha (h v - E_g)$$
 (5)

The optical direct bandgap of $(\alpha hv)^2$ vs (hv) is plotted to be graph fig.4 (c)



The refractive index measurehow much light slows down and bends as it travels through a material, reflecting the optical density and transparency of the crystal. At 532nm, the crystal exhibited a linear refractive index (no) of 0.02, indicating moderate light-matter interaction suitable for optical and nonlinear optical applications.

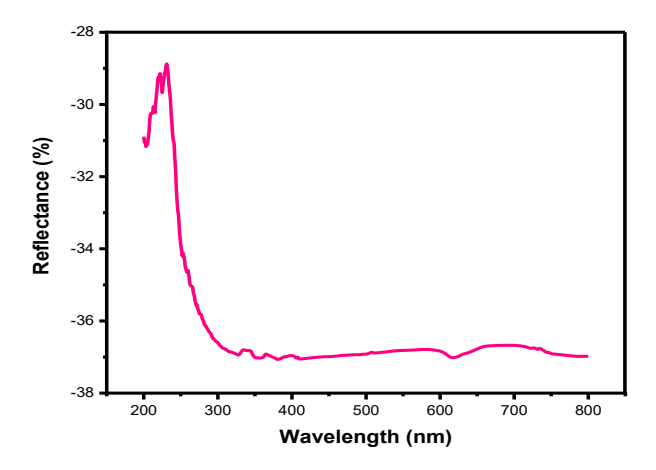


Fig. 4(d) Wavelength vs Reflectance

Reflectance measurements in the ultro violent region were conducted to evaluate optical properties for the sample.

The formula for Reflectance is.

$$R = 1 \pm \sqrt{1 - \exp(-\alpha t)} + \exp(\alpha t) / 1 + \exp(-\alpha t)$$
 (6)

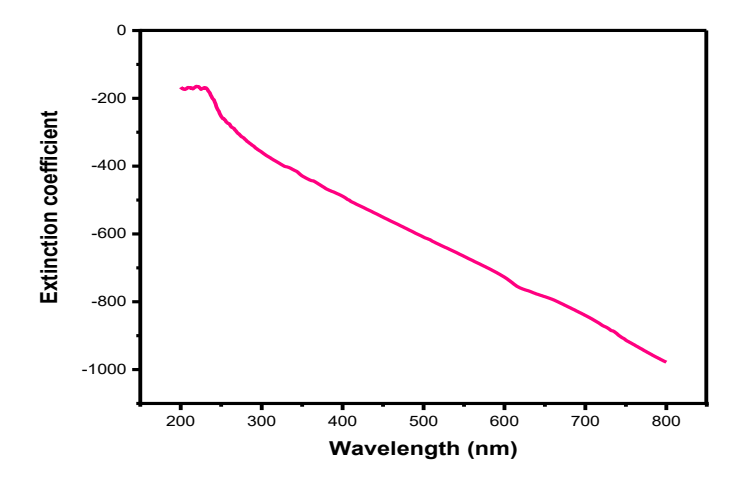


Fig. 4(e) Wavelength versus Extinction coefficient

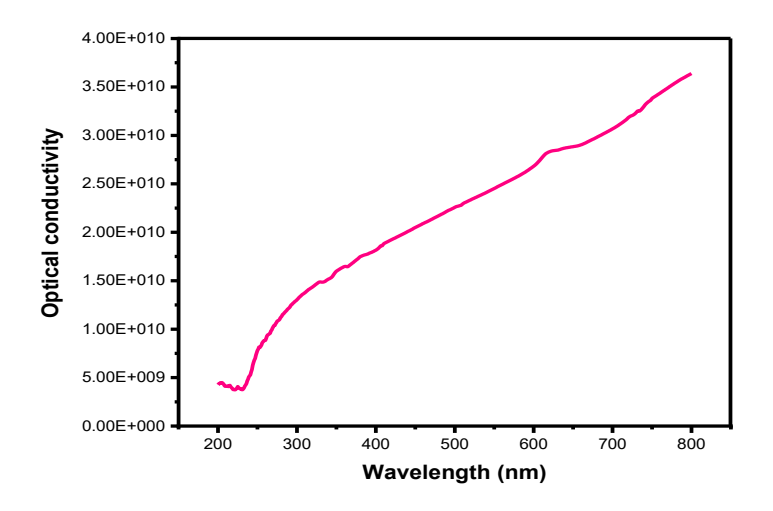


Fig. 4(f) Wavelength versus Optical conductivity

The equation determine the Extinction coefficient is

$$\mathbf{K} = \lambda \alpha / 4\pi \tag{7}$$

Refractive index (n_o)was determined using the established relation

$$n_0 = -(R+1) 2 \sqrt{Nr / (R-1)}$$
 (8)

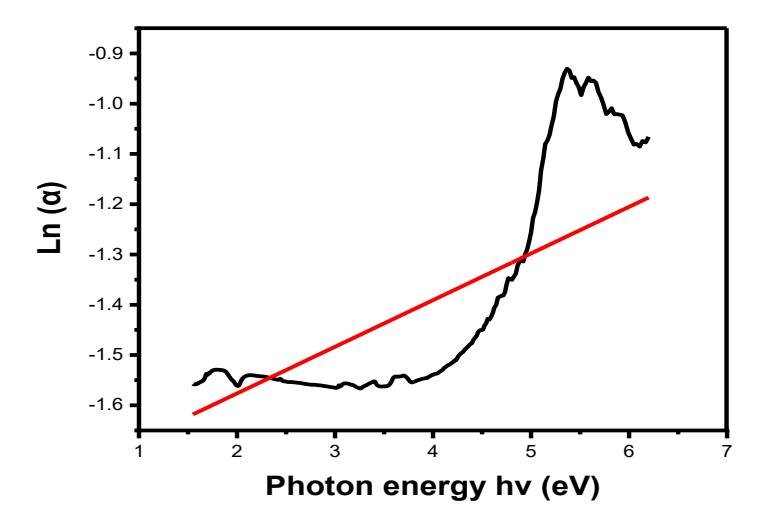


Fig. 4(g) Urbach energy plot

The Urbach rule (E_u) equation is

$$\alpha = \alpha_0 e \text{ hv/E}_u \tag{9}$$

Taking Log on both sides

$$\ln \alpha = \ln (\alpha_0) + hv/E_u$$
 (10)

By Plotting $ln\alpha versus$ Photon energy hv (eV), the urbach energy is calculated from the inverse of the slope

$$E_{u} = 1 / Slope \tag{11}$$

Optical absorption edge of the Glycine was examined usingurbach rule to estimate urbach energy (E_u), which reflects the extent of tail states within the energy band [10].

According to urbach formalism, urbach energy (Eu) corresponds to theinverse of the linear fit slope, yielding E_u is 10.77 eV.Calculatedurbach energy (E_n) suggests the existence of low-energy irregularities throughout the crystal lattice, which may influence the optical property of a material [11, 12]. This analysis provides insight into the intrinsic electronic structure and confirms the applicability of the urbach rule to these molecular crystals [13, 14].

4). Morphological analysis

SEM characterization was performed to examine the surface morphology of the grown single crystal. SEM characterization was performed to investigate surface morphology on cracks,

structural irregularities as well as growth patterns, which were characterized using a focused electron beam [15, 16]. Scanning electron images showed that the crystal surface has a good quality structure confirms the surface quality and crystal growth [17]. Fig 5(a) to 5(e) represents the SEM image of the single crystal, highlighting the surface morphology.

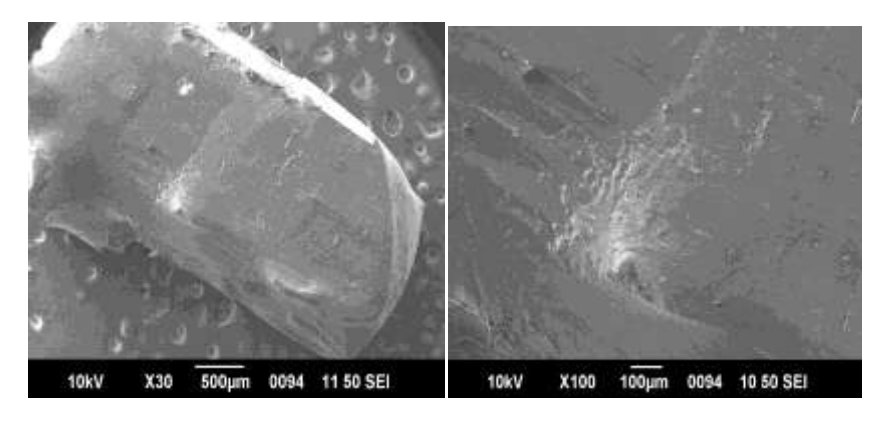


Fig. 5 (a) SEM image of the sampleFig. 5 (b) SEM image of the sample

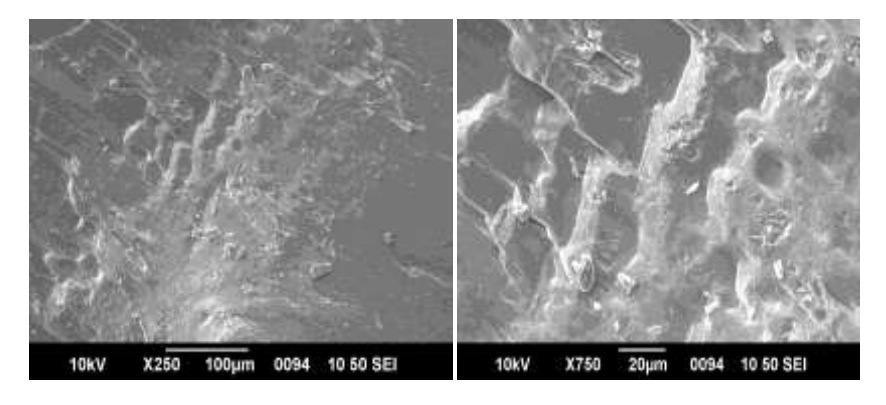


Fig. 5 (c) SEM image of the sample Fig. 5 (d) SEM image of the sample

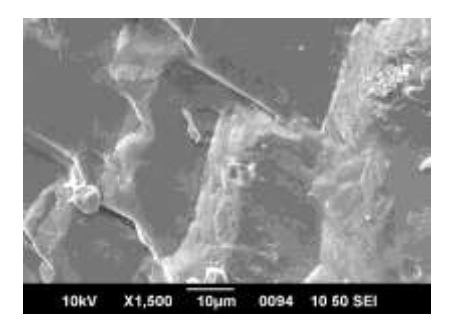


Fig. 5 (e) SEM image of the sample

5). TG DTA

In, Thermogravimetric analysis the powdered sample is weighed, and the measurement is taken as 5.175 mg. TG-DTA is a combined thermal analysis technique that simultaneously records weight changes (TG) and heat flow differences (DTA) in material with respect to temperature [18,19]. Evaluates the thermal stability window over which a material is stable before decomposition. Identifies endothermic and exothermic processes such as melting, crystallization, and oxidation [20]. In TG (ug), the initial stage decomposition occurs at 251 °C. Stage two of weight reduction occurs at398 °C and then Final step of decrease in weight at 689 °C. As the temperature increases, processes such as moisture evaporation, decomposition or oxidation may occur, leading to a reduction in mass [21, 22]. In DTA graph the minute Endothermic peak produced at 155 °C, a Majour endothermic transitionis identified around 287°C, an Exothermic transitionoccurs near 358°C, Followed by another Exothermic transition near 417 °C, accompanied by a distinct Exothermic peak around 684 °C.

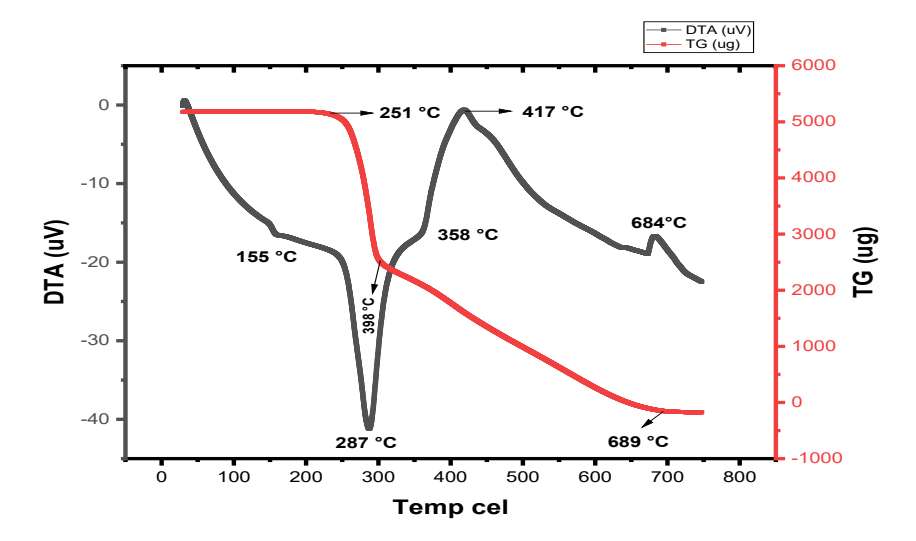


Fig. 6 (a) TG-DTA curves of Glycine A.R

Both Broido's and Kissinger the Relations are

In
$$[In (1/Y)] = Ea / R. 1/T + constant$$
 (12)

Standard Entropy of activation

 $\Delta S = 2.303R \log Ah/KT_m J/mol(13)$

Standard enthalpy of activation

 $\Delta H = E - 2RT J/mol(14)$

Standard Gibbs free energy of activation

$$\Delta G = \Delta H - T\Delta S J/mol$$
 (15)

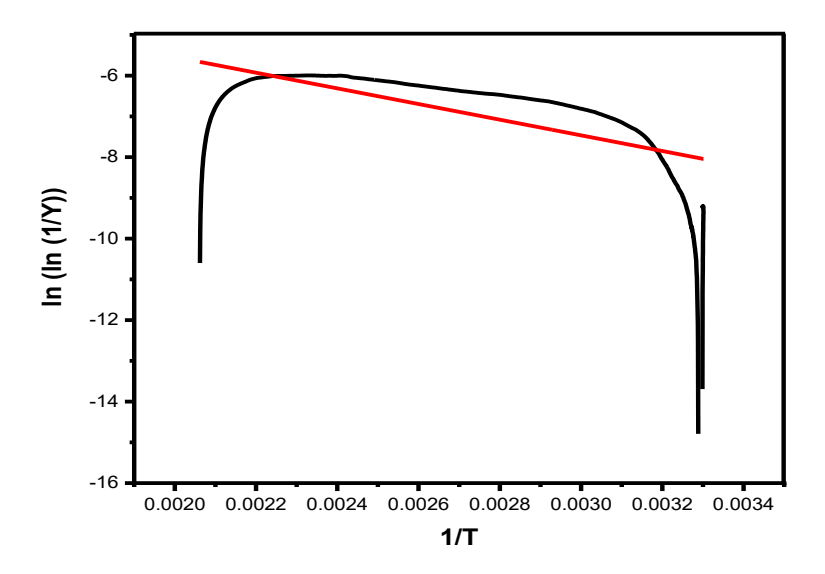


Fig. 6(b) Shows the broidos method 1/T versus Ln(ln (1/Y))

Table.4 Thermal parameters of the crystals were evaluated using the Broidos method from TG-DTA

Thermal parameters	Values
Temperature	325.176 K
Slope	1921.29954
$E_{a}(J)$	15963.99
Entropy [ΔS] (J/mol.k)	-220.8
Enthalpy [ΔH] (J/mol)	13259
Gibbs Free energy [ΔG] (J/mol)	85072

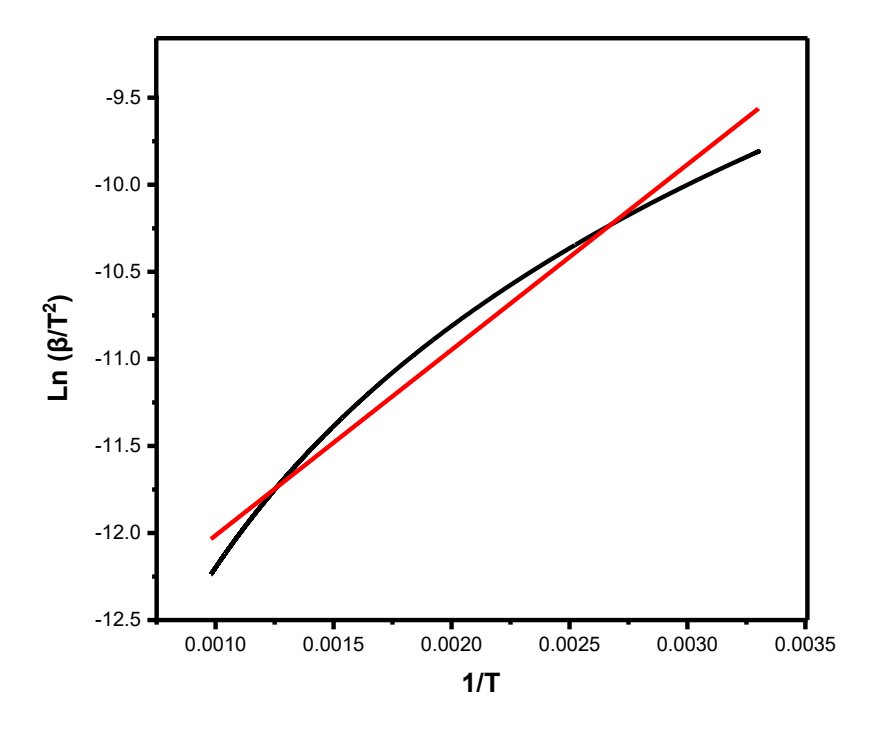


Fig. 6 (c)Shows the Kissinger method 1/T versus $Ln(\beta/T^2)$

Table. 5 Thermal parameters of the crystals were evaluated using kissinger method from TG-DTA

Thermal parameters	Values	
Temperature	527.644 K	
Slope	-1065.04502	
$E_{a}(J)$	8856.08	
Entropy [Δ S] (J/mol.k)	-296.3	
Enthalpy [ΔH] (J/mol)	4475.1	
Gibbs Free energy [ΔG] (J/mol)	160571.6	

The thermal decomposition kinetics of the studied nonlinear optical (NLO) crystal were analyzed using both Kissinger and Broidos methods based on TG-DTA data[23]. The results revealed that the calculated activation energy, Enthalpy, and entropy of activation varied depending on the method, reflecting differences in the kinetic and thermodynamic interpretations of the decomposition process. Both methods indicated negative entropy of activation values, suggesting an increased degree of order in the activated complex[24]. The enthalpy values derived from the Kissinger and Broido methods showed noticeable variation, highlighting the influence of the kinetic model and analytical approach on the evaluation of the material's thermal behaviour. The corresponding Gibbs free energy values further emphasized the relative thermodynamic favourability of the decomposition process. Overall, the combined analysis provided a complementary understanding of materialstability along with degradation behaviorin NLO samples[25].

6). Elemental analysis

For CHN elemental analysis, a sample weighing 9.09 mg was employed. This Confirms that the stoichiometry of the final crystal matches the theortical molecular formula. CHN Elemental characterization was conducted to quantify the C (%), H (%), and N (%) content in the grown crystals. CHN analysis of Glycine (A.R) reveals that the crystal contains Nitrogen (20.57 %), Carbon (34.04 %) and Hydrogen (14.01 %). The experimental observed values were in close agreement, confirming the chemical composition and purity of the crystal [26]. The molecular formula for CHN analysis is C₂H₅NO₂. Experimental results are illustrated bytable (6). A Molecular structure of Glycine A.R is presented in Figure (7).

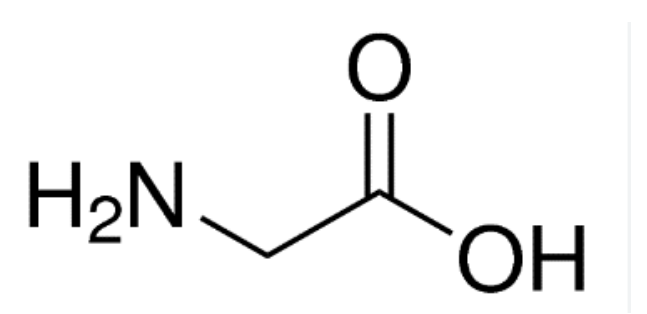


Figure. 7Molecularstructure for CHN analysis

Table.6 CHN elemental analysis results of Glycine A.R single crystals

S.NO	Samplename	Nitrogen %	Carbon %	Hydrogen %	Sample weight
1.	Glycine A.R	20.57	34.04	14.01	9.09(mg)

7). Photoluminescenes analysis

PL characterization provides a method to investigate the emission of light from a material at specific wavelengths. As electrons relax to lower energy level, energy is emitted as radiation [27]. This emitted is collected and analyzed its intensity and wavelength tell us about the electronic and structural property of the material [28]. It also reveals the bandgap of the crystal. It indicates optical quality and potential for optoelectronic applications [29]. The maximum peak obtained at 466 nm. The second peak emission produced at 538 nm. The third emission produced around 620 nm. The final peak obtained at 822 nm.

Energy bandgap for Photoluminescenes analysis is determined using the following equation is

$$E_{g} = hc/ke \tag{16}$$

The bandgap value is calculated to be is 2.66 eV.

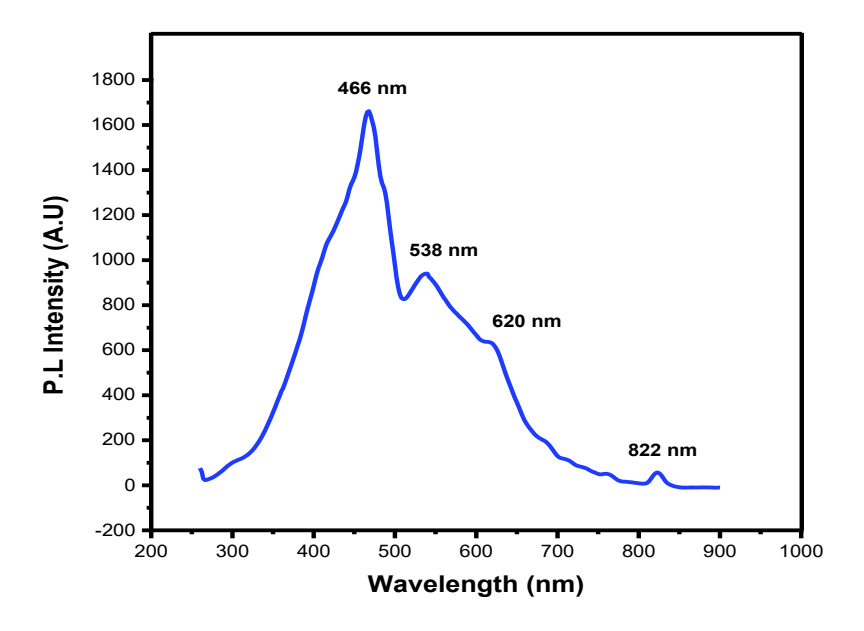


Figure.8 Photoluminescence spectra of Glycine A.R single crystals

The observed photoluminescence emission at 2.66 eV (466 nm, Blue region) demonstrates the material's potential in Nonlinear optics, particularly inSHG, frequency conversion, optical switching and Photonic device fabrication [30].

8).EDAXtechnique

Energy dispersive x-ray characterization can be usually attached to an SEM (Scanning electron microscope). When the electron beam interacts with the specimen, it ejects inner shell electron from atoms [31]. The atom becomes unstable, causing a charged particle in an upper energy level to move into the vacant position, emittingX-radiation. Through measurement of X-ray energies, the constituent elements in the material can be identified. EDAX is mainly helps to identify the percentages of weight (%) and Atom (%). The Carbon, Nitrogen and Oxygen are the lighter elements are observed in the K-Shell series. A grown crystal of Glycine A.R has the presence of three lighter elements present they are Carbon, Hydrogen and oxygen[32]. The Elements percentages are mentioned in the table. (7). The EDX high resolution image was recorded in Fig 9 (a) & 9 (b).



Fig.9 (a) EDX spectrum of the crystal

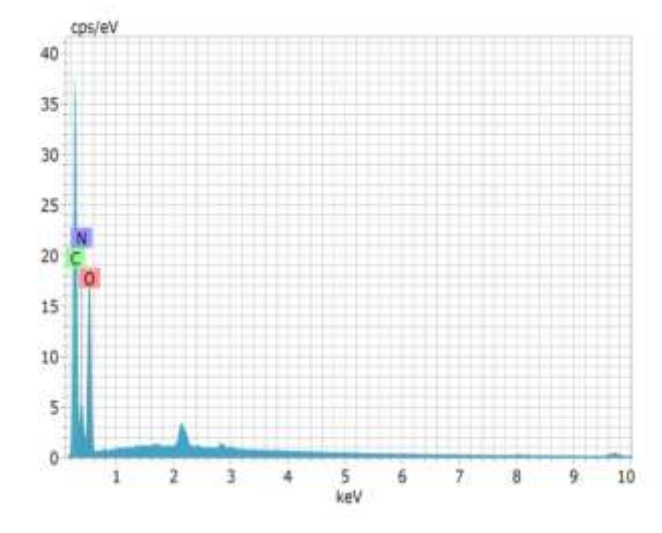


Fig. 9 (b) EDX graph of the crystal

Table. 7 EDAX analysis of Glycine A.R showing the elemental composition with various percentages

Element [wt.%]		unn. C [at.%]		Atom. C	Error (3 Sigma)
Oxygen	K-series	38.8538.85	33.44	14.40]	
Carbon	K-series	39.26	39.26	45.03	13.82
Nitrogen	K-series	21.89	21.89	21.53	9.40
Total:		100.00	100.00	100.00	

9). LDT

The LDT is defined as the maximum laser fluence or intensity that a material can tolerate without undergoing permanent damage. This represents a critical property of sampleutilized for Photonic and laser based devices. LDT depends on factors such as Laser wavelength, Pulse duration, Beam size, and Repetation rate. High LDT materials are preferred for optical lenses and nonlinear optical crystals to ensure stability under intense laser irradiation. Measuring LDT provides insight into a material's optical, Thermal, and Structural properties. It also helps in selecting suitable materials for High-power laser applications [33].

The LDT of the synthesized crystal was assessed with a Q-switched Nd:YAG laser at 1064 nm wavelength and a pulse duration of 10ns. A Repitation rate at 10Hz. A laser beam with a diameter 1mm, incident upon the sample surface, and the threshold energy at which surface damage occured was recorded [34, 35].

The P (d) equation is

$$P(d) = E(p) / \tau \pi(\omega o)^2$$
 (17)

The energy power was observed as 19.5 mJ

The LDTfor Glycine A.R was measured as 22.2 GW/cm². This measured Laser damage thresholdresult demonstrates that the material can withstand high-intensity laser irradiation. The material is a promising applications used for Laser, optical and photonic devices.



Fig 10 (a). Photographic image of LDT Glycine A.R (Before)

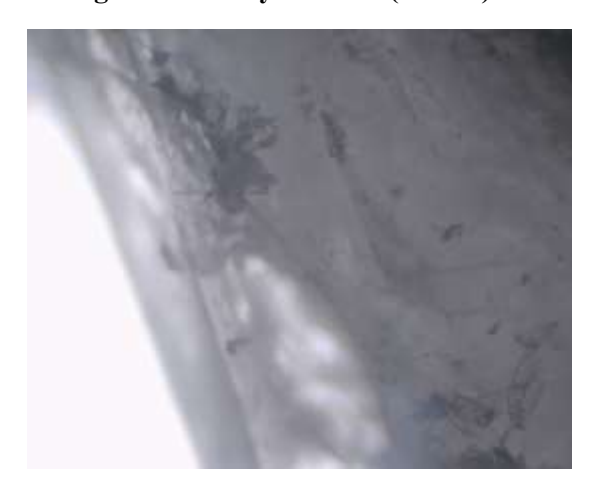


Fig 10 (b). Photographic image of LDT Glycine A.R

Table: 8

Sample	Output energy (Milli joule)	LDT values (GW/cm²)
Glycine A.R	19.5 mJ	22.2

10). ¹H FT NMR

¹H FT-NMR to the nucleus of hydrogen (Proton). In NMR spectroscopy, ¹H is the most commonly studied nucleus because almost all organic compounds contains hydrogen [36]. A FT-NMR is the technique that uses for a strong magnetic field that probe the magnetic properties of atomic nuclei, providing insights into the chemical structure. FT-NMR provides information on the molecular structure and chemical interactions [37].

The Glycine single crystals in ¹H FT-NMR signals peak appear around 3.283 ppm corresponding to the group of (-CH₂) (Methylene protons) [38, 39]. The experimental obtained graph showed in fig (11).

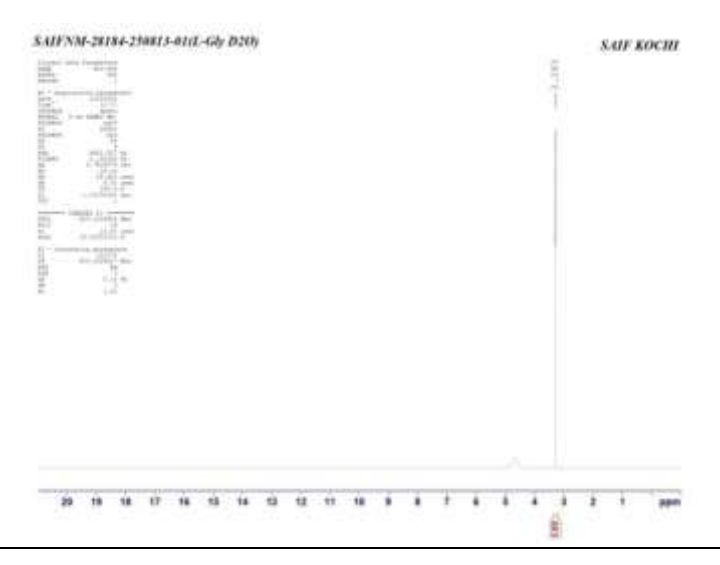


Fig. 11. ¹H FT-NMR spectrum of Glycine

11). Powder Z-scan technique

Z-scan is a experimental method is employed to measure the nonlinear optical characteristics in materials. In this method, a focused laser beam passes through the material, which is translated along the propagation axis(z-axis) across the beam's focal region. Z-scan is a simple and highly sensitive method for studying NLO properties, where changes in the transmitted light intensity are measured as a function of the sample'sposition along the propagation axis. This single-beam method allows determination of thenonlinear absorption(β) and refractive properties by moving the sample through the focal region of a focused laser beam.

Z scan characterization is employed to investigate the nonlinear optical properties of crystals, which can be analyzed in two aspects they are Nonlinear refractive index (n_2) and Nonlinear absorption coefficient (β) . Its especially common in studying material for laser

applications [40]. In this method, a laser beam is focused through a lens, and the sample is moved along the beam's propagation direction (known as the z-axis) through the focal region. As the sample travels through different positions relative to the focal point, variations in the transmitted light intensity are recorded using a detector. In, Open aperture (OA) Z scan configuration, the detector is used without an aperture to measure nonlinear absorption phenomena, such as two photon absorption. In closed aperture before the detector blocks some of the light [41]. The curve pattern denotes the valley to peak is the hallmark of self defocusing (n_2 <0) in a nonlinear optical material. Otherwise peak to valley the curve determines the self focusing (n_2 >0). The sample had a thickness of 1mm, while the calculated Rayleigh length (ZR) was 0.335 mm. Asample is positioned along the beam propagation direction, extending from -Z to +Z, with the Rayleigh length ZR < L, indicating a tightly focused beam within the medium [42].

The Open aperture to the Absorption coefficient (β)3.10 x 10⁻⁶m/W is calculated. The closed aperture to the (n_2) is observed as 1.72 x 10⁻¹³m²/W. The Real part Re ($X^{(3)}$) is found to be 1.75 x 10⁻¹⁵esu. The imaginary part Img ($X^{(3)}$) is 1.33 x 10⁻¹³ esu and finally the purpose of Z-scan method is to investigate the magnitude of third order susceptibility $X^{(3)}$ is 1.33 x 10⁻¹³esu. The NLO applications of Z scan is design of Photonic devices such as optical switches, modulators, waveguides, optical computing circuits and quantum computing circuit.

The transmittance peak (T_p) is 0.999 and Transmittance valley (T_v) is 0.030 measured from the open-aperture (β) Z-scan, yielding a ΔT_{min} of 0.970

The Transmittance peak (T_p) of 1.054 and a Transmittance valley (T_v) of 0.845 obtained from the closed aperture (n2) Z-scan, giving a $\Delta_{T_{p-v}}$ of 0.659

The open-aperture Z-scan profile exhibits a symmetric valley type curvearound the focal plane (z=0), characteristic of reverse saturable absorption (RSA), with a positive nonlinear absorption ($\beta > 0$). This behaviour, resulting from enhanced absorption under elevated light intensities, likely due to excited-state absorption or multiphoton phenomena, demonstrates the material's suitability for optical limiting applications.

The closed aperture Z-scan profile exhibits a valley to peak configuration around the focal point (z=0), demonstrating a positive nonlinear refractive index coefficient (n2>0) and confirming self-focusing behavior in the material [43].

Table (9), illustrates the corresponding valuesobtained from this experimental method. Evalution of the Open aperture curve indicates a valley type curve, as shown in figure .12 (a). The closed aperture Z-scan trace exhibits a transition from valley to peak, as illustrated in figure .12 (b).

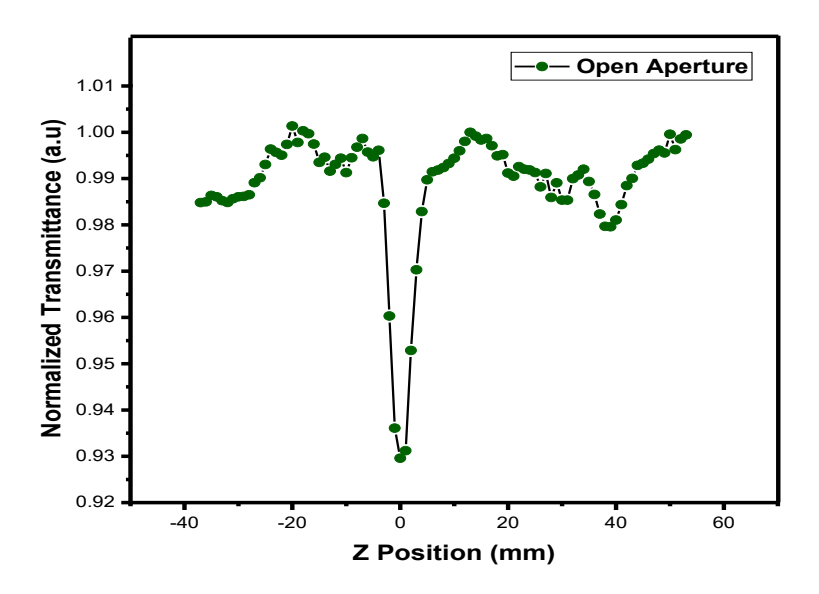


Fig. 12. (a) Open aperture Glycine A.R

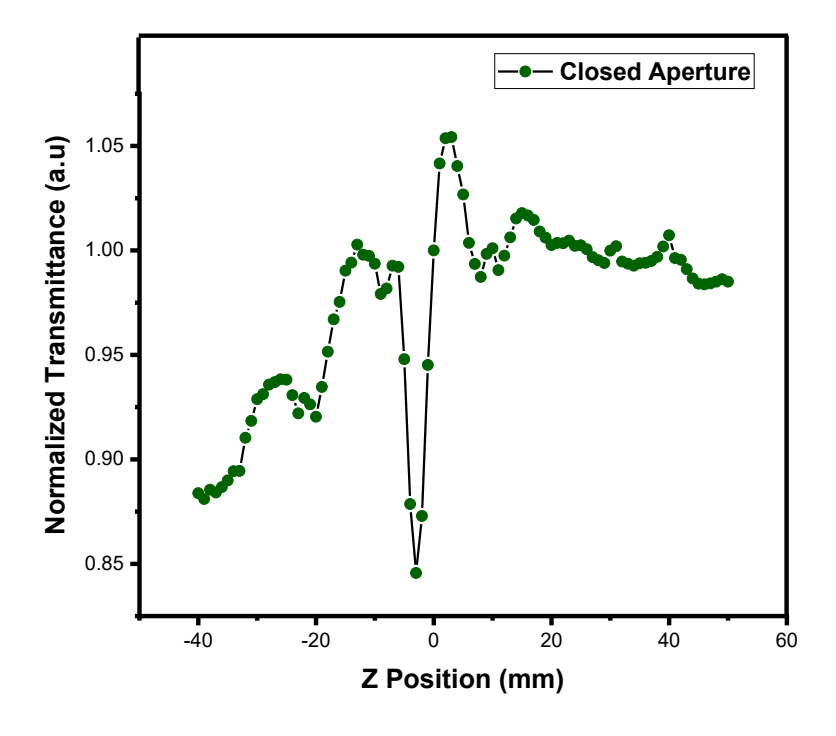


Fig. 12. (b) Closed aperture Glycine A.R

Beam characteritics	Values
Laser beam Wavelength (λ)	532 nm
Power of the laser (E _p)	100 mW
Diameter (D)	9 mm
Lens focal length (f)	20 cm
Radius of the aperture (ra)	2 mm
Beam radius of the aperture (ω_a)	4.5 mm
Z scan sample thickness (L)	1 mm

Table: 9 Illustrates the corresponding values obtained from this experimental method

12). Antibacterial Activity

Antibacterial activity refers to the ability of a substance to inhibit the growth of or kill bacteria. In crystal growth studies, this property is evaluated to understand the interaction of the grown crystals with bacterial strains. It is commonly assessed using methods such as the agar well diffusion test, where the presence of a clear inhibition zone around the sample indicates its antibacterial effect[44].

The antibacterial activity of Glycine A.R single crystals was evaluated against staphylococcus aureus (S. Aureus) and Escherichia coli (E. coli) using the agar well diffusion method. No visible zone of inhibition was observed for either bacterial strain, indicating the absence of antibacterial activity. This results suggest that the glycine A.R crystal exhibits no antibacterial effect under the tested conditions. The lack of inhibition may be attributed to the chemical stability and non-reactive nature of the glycine lattice, which limits its interaction with bacterial cell membranes [45]. Table (10). Summarizes the antibacterial activity, showing the zone of inhibition and control plate results for various bacterial strains. The antibacterial activity against staphylococcus aureus and Escherichia Coli is illustrated in Figure. (13).



Figure. 13Photograph showing antibacterial plates of the grown Glycine A.R single crystal

S. NO	Strain	Gram reaction	Control	Zone of inhibition (mm)
1	S. aureus	+Gram	25	
2	E. coli	-Gram	25	

Table: 10 Zone of inhibition and control plate results against different bacterial strain

13). Microhardness

The microhardness technique is employed to analysis the mechanical property of the synthesizedmaterial. The well flat polished surface face is (001). The microhardness 'n' value is determined through the relation given below

$H_v = 1.8544 \text{ P/d}^2 \text{ (kg/mm}^2\text{) (18)}$

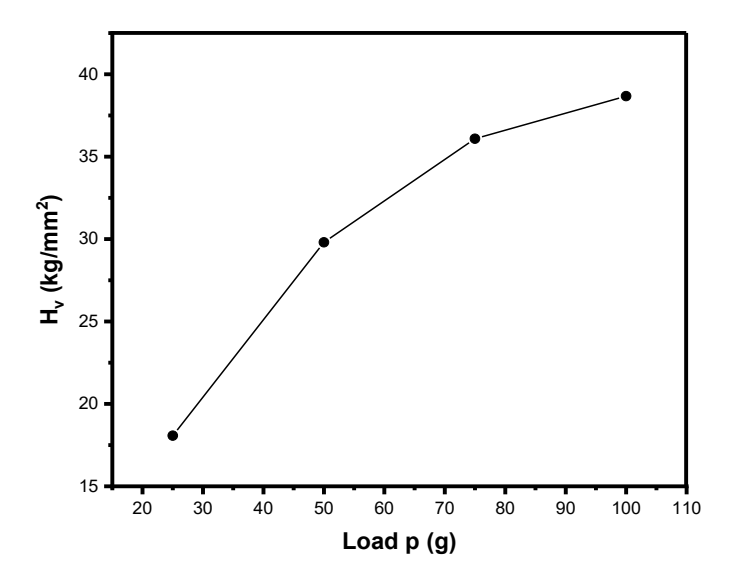


Fig. 14 (a) Load P (g) versus Hv (kg/mm²)

Thegraph of applied load (P) versus vickers hardness (H_v) in kg/mm²reveals that the resistance of the sample rises as the applied load increases, indicating a direct correlation between load and hardness behaviour. This indicates a positive correlation of the applied load and material hardness, consistent with the normal indentation size effect (ISE), where larger loads produce

larger indentations but higher measured hardness values. The various Load P(g) and Hardness (H_v) are observed in fig. 14 (a)

Mayer's hardness exponent(n)was evaluated from the slope of the logarithmic plot using the following equation



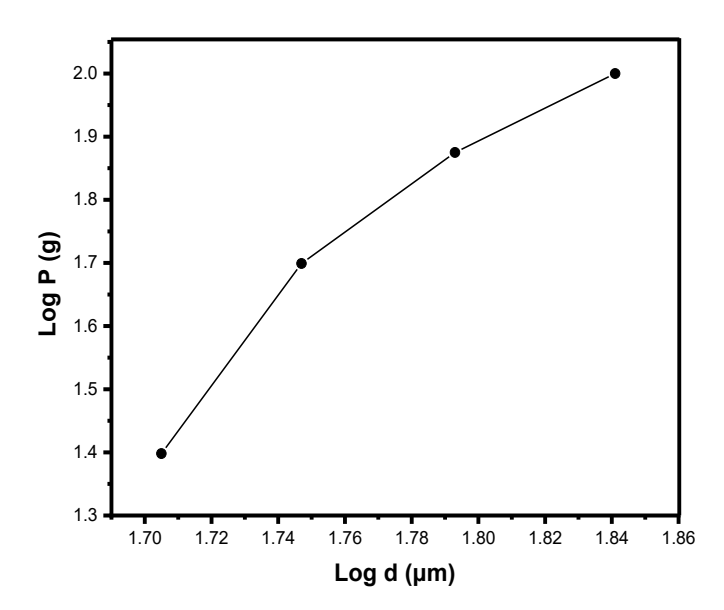


Fig. 14 (b) Log P (g) vs Log d (μm)

During the test, the material exhibits an increase in hardness (Hv) with increasing applied load (P)[46]. There are several grams of various loads are applied 25 gm, 50 gm, 75 gm and 100 gms for an time duration is 10s. Vickers microhardness measurements indicate an increase in crystal hardness as the applied load rises from 25, 50, 75 and 100 g, with corresponding indentation diagonals varying from 50.66 to 69.27 µm. The value of microhardness 'n' value found is to be 4.33. The hardness measurements were analyzed to investigate the Rise indentation size effect (RISE) of the material [47]. These results indicate that the indentation depth expands with rising applied load, illustrating the material's response under varying loading conditions. According to the onistch rule, if the obtained mayer's index value n >2, it indicates it indicates the material is classified as the hard material [48, 49]. However fluctuations at higher loads suggest possible surface. figure. 14 (b) presents the mayer index graph.

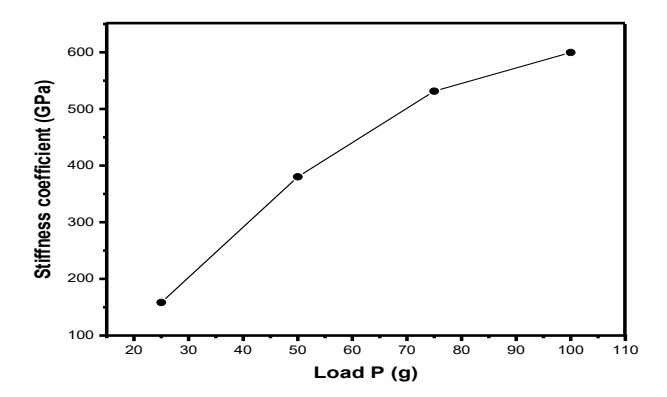


Fig. 14 (c) Load (P) vs Stiffness coefficient

The elastic stiffness coefficient (C_{11}) corresponding to various applied loads determined by the wooster's empirical relation, and its dependence on loads was examined

$$C_{11} = (H_v)^{(7/4)}GPa$$
 (20)

The material's stiffness coefficient shows a continuous increase with increasing applied load, starting from a lower value at small loads and reaching a higher value at maximum load [49]. This trend indicates that the material becomes progressively more rigid under higher loads, reflecting its ability to withstand deformation as the applied load increases.

The material's yield strength (σy) is calculated from the Vickers hardness number (Hv) using the empirical formula is,

$$\sigma y = (H_v)/(n-1) \text{ MPa (21)}$$

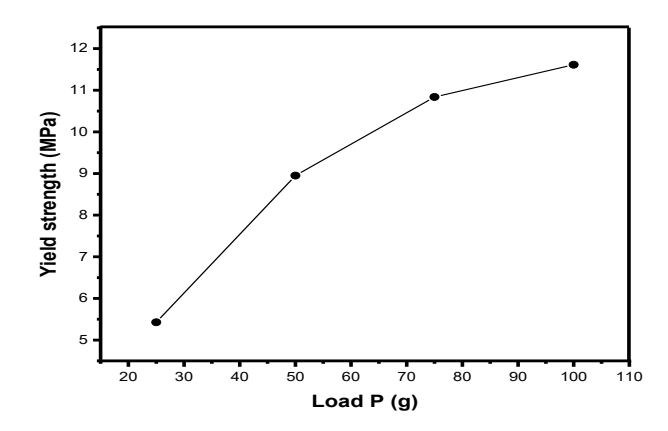


Figure. 14 (d) Load (P) vs Yield strength (MPa)

The yield strength of the material also shows a clear increase in magnitude with increasing applied load. This behavior suggests that the material can withstand higher stress before yielding, demonstrate an enhanced ability to resist plastic deformation under larger loads. The observed trend is consistent with the load-dependent strengthening behavior of the material [50].

Conclusion

Glycine A.R was synthesized at room temperature and analyzed by various characterization technique to find the structural, optical, thermal, mechanical behaviour. Powder XRD analysis reveals that the P2₁/c space group has a monoclinic crystal structure. and the diffracted peaks were indexed to their corresponding (h k l) planeswith the help of JCPDS database. In, FTIR analysis the functional group and variety of assignment are mentioned. UV-vis analysis the mainly characterized for Absorbance, Transmittance (%) and Direct Bandgap is 4.58 eV. In additionally the optical properties, including Refractive index (n_o), reflectance (%), Extinction coefficient, urbach energyand Optical conductivity UV-vis spectral data. The results confirm the material's suitability for optoelectronic applications. EDAX analysis confirmed the atomic constituents and the qualityfor the synthesizedGlycine A.R crystals. TG-DTA studies revealed heat resistance and thermal degradation for this sample. Thermal parameters were calculated using the Broido's and Kissinger method based on TG/DTA analysis CHN elemental analysis further verified the stoichiometric composition of the crystals. SEM studies revealed the material's surface morphology and microstructural features. The PL spectrum the highest peak obtained at (466 nm) which has a bandgap energy of 2.66 eV. Z-scan characterization the Nonlinear absorption (β) is 3.10 x 10⁻⁶ m/W, Nonlinear refractive index (n₂) is 1.72 x 10⁻¹³ m^2/W and then Real part Re ((X)³) is 1.75 x 10⁻¹⁵esu, then the Imaginary part Img ((X)³) is 1.33 x 10^{-13} esu and the magnitude of third order susceptibility (X⁽³⁾) is 1.33 x 10^{-13} esu. ¹H FT NMR with characteristic chemical shifts in ppm, confirmed the existence of the expected functional group and validated the compound's molecular structure. The material exhibit LDT of 22.2 GW/cm². Vickers microhardness analysis gives a mayer's index 'n' is 4.33, indicating that the crystal is classified as a hard material, suitable for nonlinear optical applications. The antibacterial study of Glycine A.R single crystals confirmed that the material exhibits no inhibitory effect against both Gram-positive and Gram-negative bacteria.

Acknowledgement

I Sincerely thank my guide Dr. K. Balasubramanian, The M.D.T Hindu college, Tirunelveli for his valuable guidance and support throughout this research work.

References

[1]. K. Ambujam, S. Selvakumar, D. Prem Anand, G. Mohamed, and P. Sagayaraj, Crystal growth, Optical, Mechanical and Electrical properties of organic NLO Material γ -Glycine, Cryst. Res. Technol. 41, No. 7, 671 – 677 (2006)

DOI: 10.1002/crat.200510647

[2]. A. Arputha Latha, M. Anbuchezhiyan, C. Charles kanagam, K. Selvarani, Synthesis and characterization of γ-glycine–a nonlinear optical single crystal for optoelectronic and photonic applications, Materials Science-Poland, 35(1), 2017, pp. 140-150

DOI: 10.1515/msp-2017-0031

[3]. V. Vijayalakshmi, P. Dhanasekarana, Growth and characterization of γ -glycine single crystals for photonics and optoelectronic device applications, Journal of crystal growth, 506 (2019) 117-121.

https://doi.org/10.1016/j.jcrysgro.2018.09.048

[4]. A. Sundari, S. Manikandan, Growth and characterization of NLO single crystal (Glycinium oxalate), Asia Pacific Journal of Research, Vol. I. Issue L, April 2017

ISSN (Online): 2347-4793

- [5]. Dr. Jyotsna, R. Pandey, Growth and optical properties of organic GOA crystals, American Journal of Engineering Research (AJER), Volume-03, Issue-03, pp-30-36,
- [6]. R. Ashok kumar, R. Ezhil Vizhi, N. Vijayan, D. Rajan Babu. Structural, dielectric and piezo electric properties of nonlinear optical γ-Glycine single crystals. Physica B, 406, (2011) 2594-2600.

DOI: 10.1016/j.phyb.2011.04.001

[7] T. P srinivasan, R. Indirajith, R. Gopalakrishnan, Growth and characterization of α and γ -Glycine single crystals, Journal of crystal growth, 318 (2011) 762-767.

DOI: 10.1016/j.jcrysgro.2010.11.117

- [8]. T. Baraniraj, P. Philominathan. Growth and Characterization of Gamma Glycine Single Crystals Grown from Alpha Glycine in the Presence of Sodium Acetate. Journal of Minerals & Materials Characterization & Engineering, Vol. 10, No.4, pp.351-356, 2011
- [9]. Sarath Ravi, Rakhi sreedhran, K. R. Raghi, T. K. Manoj kumar, K. Naseema, Experimental and computational perspectives on linear and non linear optical parameters of an orthorhombic crystal for optical limiting applications, Applied physics A Material science and processing, (2020) 126:56

DOI: https://doi.org/10.1007/s00339-019-3234-0

[10]. Rakhi sreedharan, sarath Ravi, K.R. Raghi, T.K. Manoj kumar, K. Naseema, Growth, Linear-Nonlinear optical studies and quantum chemistry formalism on an organic NLO crystal

for opto-electronic applications experimental and theoretical approach, SN Applied sciences (2020) 2:578

DOI: https://doi.org/10.1007/s42452-020-2360-9

[11]. Vincent Crasta, V. Ravindrachary, R.F. Bhajantri, Richard Gonsalves, Growth and characterization of an organic NLO crystal: 1-(4-methylphenyl)-3-(4-methoxyphenyl)-2-propen-1-one, Journal of Crystal Growth 267 (2004) 129–133

DOI: 10.1016/j.jcrysgro.2004.03.037

[12]. P. Karuppasamy, Muthu senthil pandian, P. Ramasamy, Sunil verma, Crsytal growth, structural, Optical, thermal, mechanical, Laser damage threshold and electrical properties of triphenylphosphine oxide 4-nitrophenol (TP4N) single crystals for nonlinear optical applications. Journal of optical materials, 79 (2018) 152-171.

DOI: https://doi.org/10.1016/j.optmat.2018.03.041

- [13]. M. Narayan Bhat, S. M. Dharmaprakash. New nonlinear optical material: glycine sodium nitrate. Journal of Crystal Growth 235 (2002) 511–516
- [14]. M. Anbu arasi, M. Alagar, M. Raja pugalenthi. Synthesis of Y-Glycine-NLO active single crystals via assisted of Lithium iodide and L-Proline template and determination of micro-structural and optical parameters. Journal of Materials letters. 274 (2020) 128044.

DOI://doi.org/10.1016/j.matlet.2020.128044

[15]. B. Deepa, P. Philominathan, Investigation on the optical, mechanical and magnetic properties of organic NLO single crystal: Pyridine 3-carboxylic acid, Optik – international journal forlight and electron optics, (2016).

DOI: http://dx.doi.org/10.1016/j.ijleo.2016.06.073

[16]. Redrothu, Hanumantha Rao, S. Kalainathan, Spectroscopic investigation, nucleation, growth, optical, thermal, and second harmonic studies of novel semi organic nonlinear optical crystal-Thio urea urea zinc sulphate, Spectrochimica Acta Part A: Molecular and Biomolecular Spectroscopy,

97 (2012) 456-463.

DOI: http://dx.doi.org/10.1016/j.saa.2012.06.033

[17]. S. Arockia Avila, A. Leo Rajesh. Growth and characterization of L-Glycine sodium nitrate single crystal for electro-optic applications. International journal of scientific research in science and technology (IJSRST). Volume 3, Issue 11, pp.43, November-December 2017. Presented at: Int. conference on advanced materials (ICAM-2017), St. Joseph college, Trichy, India. [Online]. Available: https://www.ijsrst.com

[18]. M. Lakshmipriya, R. Ezhil vizhi, D. Rajan Babu, Growth and characterization of maleic acid single crystal, Optik 126 (2015), 4259-4262

DOI: http://dx.doi.org/10.1016/j.ijleo.2015.08.126

[19]. N. N. Shejwal, Mohd Anisy, S. S. Hussainiz and M. D. Shirsat, Investigation on structural, UV-visible, SHG efficiency, dielectric, mechanical and thermal behavior of L-cystine doped zinc thiourea sulphate crystal for NLO device applications, International Journal of Modern Physics B, Vol. 30, No. 0 (2016) 1650159

DOI: 10.1142/S0217979216501599

- [20]. P. Suresh, R. Sugaraj Samuel, S. Janarthanan, An Investigation on the Growth and Characterization of L-Tryptophan Single Crystal, Materials Today: Proceedings 5 (2018) 14225–14229
- [21]. P. Selvarajan, J. Glorium Arul Raj, S. Perumal. Characterization of pure and urea-doped γ- Glycine single crystals grown by solution method. Journal of crystal growth. 311 (2009) 3835-3840.

DOI: 10.1016/j.jcrysgro.2009.05.014

- [22]. T. Thaila and S. Kumararaman. Growth and characterization of Glycine magnesium chloride single crystals for NLO applications. Archives of Applied Science Research 2012, 4 (3): 1494-1501
- [23]. S. Radhika, C. M. Padma, A. Jeya Rajendran, S. Ramalingam, T. Chithambara Thanu. Thermal, optical, mechanical and dielectric properties of a novel NLO active Glycine potassium sulphate single crystals. Der pharma Chemica, 2012, 4(5): 2014-2023.
- [24]. G. R. Dillip, P. Raghavaiah, K. Mallikarjuna, C. Madhukar Reddy, G. Bhagavannarayana, V. Ramesh kumar, B. Deva Prasad Raju. Crystal growth and characterization of Glycine grown from potassium fluoride for photonic applications. Spectrochimica Acta Part A:MMolecular and Biomolecular spectroscopy. 79 (2011) 1123-1127.

DOI: 10.1016/j.saa.2011.04.031

[25]. P. Sagunthala, V. Veeravazhuthi, P. Hemalatha & P. Yasotha. A study on the growth and characterization of zinc sulphate mono hydrate doped glycine NLO single crystals, Ferroelectrics, 504:1, 96-103, (2016).

DOI: 10.1080/00150193.2016.1239487

[26]. S. Manikandan, R. Mahalakshmi, P. Krishnan, F. Yogam, P. Rajesh, Growth, structural, Optical, thermal and dielectric properties of L-Asparagine monohydrate admixtured L-thiomalic acid single crystal, Optik, (2016)

DOI: https://dx.doi.org/10.1016/j.ijleo.2016.03.036

[27]. M. Paul, Dinakaran, S. Kalainathan, Synthesis, nucleation, growth, structural, spectral, thermal, Linear and Non linear optical studies of novel organic NLO crystal: 4-fluoro 4-nitrostilebene (FONS), Spectrochimica Acta Part A: Molecular and Biomolecular Spectroscopy, 105 (2013) 509-515.

DOI: http://dx.doi.org/10.1016/j.saa.2012.12.050

[28]. S. Sindhusha, C.M. Padma, B. Gunasekaran, H. Marshan Robert, Structural, optical and thermal analysis of creatininium borate e A new semiorganic nlo single crystal, Journal of Molecular Structure 1209 (2020) 127981

DOI: https://doi.org/10.1016/j.molstruc.2020.127981

[29]. Mohd Anis, S. P. Ramteke, M. D. Shirsat, G. G. Muley, M. I. Baig. Novel report on Y-Glycine crystal yielding high second harmonic generation efficiency. Journal of optical materials. 72 (2017) 590-595

http://dx.doi.org/10.1016/j.optmat.2017.07.007

[30] N. N. Shejwal, S.S. Hussaini, Ramesh B. Kamble, Mohd Anis and M.D. Shirsat. Studies on the Structural, Thermal, Fluorescence and Linear—Non-linear Optical Properties of Glycine Sodium Acetate Single Crystal for Electro-Optic Device Applications. Recent Trends in Materials Science and Applications, Springer Proceedings in Physics, 189

DOI: 10.1007/978-3-319-44890-9 45

[31]. K. Premlatha, N.R. Rajagopalan, P. Krishnamoorthy, Contemporary studies on growth and characterization of Magnesium doped γ -glycine – A potential optoelectronic NLO material, Journal of molecular structure, 1240 (2021) 130593.

https://doi.org/10.1016/j.molstruc.2021.130593

[32]. P. Justina Angelin, P. Sumithraj Premkumar, Structural, optical, second harmonic, and mechanical studies on zinc chloride added alpha-glycine crystals, Chemistry of inorganic materials, 3 (2024) 100060.

https://doi.org/10.1016/j.cinorg.2024.100060

[33]. S. Gracelin Juliana, P. Sathishkumar, and S. C. Vella Durai. Crystal growth and characterization of an efficient Nonlinear optical material: γ-Glycine crystal. Indian Journal of Pure and applied physics. Vol. 62, December 2024, pp.1098-1105

DOI: 10.56042/ijpap.v62i12.9843

[34]. Sivasubramani Vediyappan, Arumugam Raja, Ro Mu Jauhar, Ramachandran Kasthuri, Viswanathan Vijayan, Muthu Senthil Pandian, Ramasamy Perumalsamy, and Vinitha Gandhiraj, Synthesis, crystal growth, structure, crystalline perfection, thermal, linear, and nonlinear optical investigations on 2-amino-5-nitropyridine 4-chlorobenzoic acid (1:1): a novel organic single crystal for NLO and optical limiting applications, J Mater Sci: Mater Electron (2021) 32:15026–15045

https://doi.org/10.1007/s10854-021-06056-5

[35]. N. Sivakumar, V. Jayaramakrishnan, K. Baskar, C. Anbalagan. Synthesis, growth and characterization of Y-Glycine A Promising material for optical applications. Journal of optical material 27 (2014) 780-787

DOI: http://dx.doi.org/10.1016/j.optmat.2014.09.007

[36]. S. Janarthanan, R. Sugaraj Samuel, Y. C. Rajan, S. Pandi, Growth, spectral, and thermal characterization of the NLO crystal: semi carbazone of DL-camphor (SDLC), J Therm Anal Calorim (2012) 107:1213–1217

DOI 10.1007/s10973-011-1632-4

- [37]. S. B. Patil, S. Dongare, M.M. Khandpekar, S.R. Patil and V.H. Singh. Studies in solution growth of L-Glycine doped with mixed sulphate and NLO properties. Vidyabharati International Interdisciplinary Research Journal. (Special Issue-Oct 2020). ISSN 2319-4979
- [38]. P. Prabukanthan, C. Raveendiran, G. Harichandran, Perumal Seenuvasakumaran, Synthesis, crystal growth, crystal structure, optical, thermal, biological and NLO studies of heterocyclic compound N-(1,3-benzothiazol-2-yl)-2methoxybenzamide, Results in Chemistry 2 (2020) 100083

DOI: https://doi.org/10.1016/j.rechem.2020.100083

[39]. S. Gowri, T. Uma devi, D. Sajan, S.R. Bheeter, N. Lawrence, Spectral, thermal, and optical properties of L-Triptophanium picrate: A nonlinear optical single crystal, Spectrochimica Acta part A 81 (2011) 257-260.

DOI: doi:10.1016/j.saa.2011.06.007

[40]. P. Sangeetha, D. Barathi, M. Uthayakumar, A. Dhandapani, M. Suresh, Vandana Shind, Crystal growth, structural and DFT study of novel single crystal (E)-N'-(2chlorobenzylidene)-4-fluorobenzohydrazide for nonlinear optical applications, Journal of Optical Materials,

DOI: https://doi.org/10.1016/j.optmat.2023.113569

- [41]. K. Senthil, S. Kalainathan, A. Ruban Kumar, P. G. Aravindan, Investigation on synthesis, crystal structure and third-order NLO properties of a new stilbazolium derivative crystal: A promising material for nonlinear optical devices, Journal of royal society of chemistry,
- [42]. T. Sivanesan, V. Natarajan, and S. Pandi, Nonlinear optical properties of α -Glycine single crystals by Z-scan technique. Indian journal of science and Technology, Vol. 3, No. 6 (June 2010), ISSN: 0976-6846
- [43]. P. Karuppasamy, V. Sivasubramani, M. Senthil Pandian, P. Ramasamy. Growth and characterization of semi-organic third order nonlinear optical (NLO) Potassium 3,5-Dinitrobenzoate (KDNB) single crystal. Royal society of chemistry. (2016).

DOI: 10.1039/C6RA21590D

[44]. S. Sakthy Priya, K. Balakrishnan, A. Lakshmanan, P. Surendran, P. Rameshkumar, Karthik Kannan, P. Geetha, Tejaswi Ashok Hegde, G. Vinitha, Crystal Growth and Characterization of Benzimidazolium Salicylate Single Crystal for Nonlinear Optical Studies and Antibacterial Activity, Journal of physics and chemistry of solid state, V. 21, No. 3 (2020) pp. 377-389

DOI: 10.15330/pcss.21.3.377-389

[45].S. Sakthi priya, K. Balakrishnan, P. Surrendran, A. Lakshmanan, S. Pushpalatha, P. Rameshkumar, P. Geetha, Karthik kannan, Tejaswi Ashok Hedge, G. Vinitha. Investigation on nonlinear optical and antibacterial properties of organic single crystal: p-Toluidinium L-Tartrate. Chemical Data collections 31 (2021) 100640

DOI://doi.org/10.1016/j.cdc.2020.100640

[46]. A. Senthil, T. Bharanidharan, M. Vinnila, K. Elangovan, S. Muthu, Crystal growth, Hirshfeld analysis, optical, thermal, mechanical, and third-order nonlinear optical properties of cyclohexylammonium picrate (CHAP) single crystal, Journal of Heliyon, 10 (2024) e28002

DOI://doi.org/10.1016/j.heliyon.2024.e28002

[47]. A. Mohamed Ibrahim and S. Arunachalam, Experimental and theortical perspectives on L-tryptophan: An amino acid single crystal for nonlinear optical applications, Rasayan J. Chem., 12(3), 1219-1228 (2019).

DOI: http://dx.doi.org/10.31788/RJC.2019.1235172

[48]. T. Balakrishnan, R. Ramesh Babu, K. Ramamurthi. Growth, Structural, optical and thermal properties of γ- Glycine crystal. Spectrochimica Acta Part –A. 69 (2008) 1114-1118.

DOI: 10.1016/j.saa.2007.06.025

- [49]. Sagadevan Suresh. Studies and mechanical and Electrical properties of NLO active L-Glycine single crystal. Materials physics and mechanics 16 (2013) 101-106.
- [50]. K. Balasubramanian, P. Selvarajan, Studies on the growth and various properties of triglycine sulphate (TGS) crystals doped with copper sulphate, Recent Research in science and technology, 2010, 2(3): 06-13, ISSN: 2076-5061